

# Cognitive Wireless Mesh Networks with Dynamic Spectrum Access

Kaushik R. Chowdhury, *Student Member, IEEE*, and Ian F. Akyildiz, *Fellow, IEEE*

**Abstract**—Wireless Mesh Networks (WMNs) are envisaged to extend Internet access and other networking services in personal, local, campus, and metropolitan areas. Mesh routers (MR) form the connectivity backbone while performing the dual tasks of packet forwarding as well as providing network access to the mesh clients. However, the performance of such networks is limited by traffic congestion, as only limited bandwidth is available for supporting the large number of nodes in close proximity. This problem can be alleviated by the cognitive radio paradigm that aims at devising spectrum sensing and management techniques, thereby allowing radios to intelligently locate and use frequencies other than those in the 2.4 GHz ISM band. These promising technologies are integrated in our proposed COgnitive Mesh NETWORK (COMNET) algorithmic framework, thus realizing an intelligent frequency-shifting self-managed mesh network. The contribution of this paper is threefold: (1) A new approach for spectrum sensing is devised without any change to the working of existing de facto mesh protocols. (2) An analytical model is proposed that allows MRs to estimate the power in a given channel and location due to neighboring wireless LAN traffic, thus creating a virtual map in space and frequency domains. (3) These models are used to formulate the task of channel assignment within the mesh network as an optimization problem, which is solved in a decentralized manner. Our analytical models are validated through simulation study, and results reveal the benefits of load sharing by adopting unused frequencies for WMN traffic.

**Index Terms**—Analytical Modeling, Cognitive Radio, Spectrum Sensing, Spectrum Sharing, Wireless Mesh Networks

## I. INTRODUCTION

WIRELESS Mesh Networks (WMNs) are envisaged to be a key technology that allows ubiquitous connectivity to the end user. A typical WMN consists of mesh routers (MRs) forming the backbone of the network, interconnected in an ad-hoc fashion. Each MR can be considered as an access point serving a number of users or mesh clients (MCs) [2]. The MCs could be mobile users, stationary workstations or laptops that exchange data over the Internet. They direct their traffic to their respective MRs, which then forwards it over the backbone, in a multi-hop manner, to reach the gateway that links to the Internet. Thus, WMNs promise community wide network access at affordable monetary and infrastructure costs.

While WMNs enhance performance with flexible network architectures, easy deployment and configuration, and fault tolerance, the high density of nodes may lower the network

capacity. From the analytical results in [11], it follows that the throughput capacity per node reduces significantly when the node density increases. In addition, the 2.4 GHz ISM band currently used by mesh based architectures is shared by most single access-point based Wireless Local Area Network (WLAN) devices, Bluetooth [26], radiation from microwave ovens, amongst others. Urban areas are affected most by this channel congestion [13], and thus there is a strong motivation to identify unused portions of the spectrum which can be used to carry the mesh network traffic. This effectively reduces the node density per transmission channel, thus improving throughput and can be attractive as lower frequencies, especially in the MHz range, exhibit better propagation characteristics. In this work, we use the terminology *secondary band* for the ISM band and *secondary users* for mesh network devices operating in that band.

The need for *intelligent* and *network aware* spectrum selection can be addressed by the recently emerging cognitive radio paradigm. These radios may decide transmission parameters such as channel, power, modulation type, and transmission rate through local coordination based on their perception of the surrounding environment [1]. The Federal Communications Commission (FCC) has encouraged work in spectrum sharing issues by initiating steps to free up unused portions of the spectrum and advocating the use of digital television over its analog counterpart. This may free up bandwidth in the 54 – 72 MHz, 76 – 88 MHz, 174 – 216 MHz, and 470 – 806 MHz bands [7]. We consider the more general scenario, in which the entire frequency ranges are not completely vacated, but may experience occasional transmissions by the licensed users. Also, certain frequencies may be reserved for special communication needs, such as emergency services and military, which may see a burst of network activity followed by a long duration for which the channel lies unused. We refer to these bands as *primary bands* and the licensed operators in them as *primary users* in the subsequent discussion.

In this paper we explore ways in which secondary users equipped with tunable radios may share the primary band, thus coexisting with the licensed users of that band. It is imperative that primary users in these bands have priority in communication and their operation must not be hindered by spectrum sharing techniques. Thus, the key challenges that must be addressed include identifying which portions of the spectrum are free for use, resolving contentions with the licensed users operating in those frequencies and load balancing over the entire available spectrum.

Our proposed COgnitive wireless Mesh NETWORK (COMNET) suite of spectrum sensing and sharing algorithms takes

Manuscript received March 1, 2007; revised August 24, 2007.

Kaushik R. Chowdhury and Ian F. Akyildiz are with the Broadband Wireless Networking Laboratory, School of Electrical and Computer Engineering, Georgia Institute of Technology, Atlanta, GA, 30332 USA (e-mail: kaushikc.ian@ece.gatech.edu).

Digital Object Identifier 10.1109/JSAC.2008.080115.

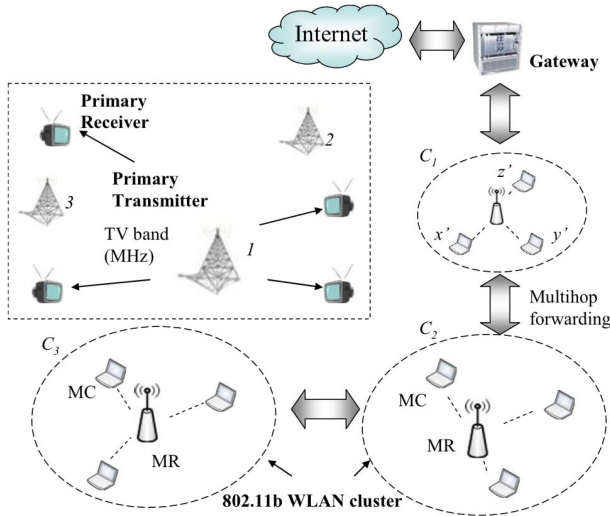


Fig. 1. Example mesh architecture with mesh routers (MRs) and mesh clients (MCs) under them. The mesh components are located in a spatially overlapped region with primary transmitter stations.

the first step in leveraging the benefits of cognitive radio technology in the area of WMNs. We adhere to the standard assumptions of WMNs [2] in terms of the nature and number of available interfaces at each mesh node, save the additional ability to transmit at either the primary or secondary band at a given time. Thus, our solution can be easily integrated into an existing mesh scenario with little change to the deployed infrastructure. Specifically, the contributions made in this paper are as follows:

- We propose a scheme that allows MCs, equipped with a single tunable transceiver, to monitor the primary channels while continuing operation in the secondary band.
- We devise a theoretical framework for identifying primary transmitter frequencies through time domain sampling. We achieve this by formulating the task of sensing as a linear programming problem based on received signal strength values on any given channel.
- While sensing is used to locate empty portions of the spectrum, it is necessary to evaluate the additional power injected before actually shifting the secondary users in the primary band. For this, we propose an analytical model of estimating interference caused at any arbitrary location and frequency due to the mesh traffic.
- We formulate the task of channel assignment as an optimization problem that is solved at each MR using the empty channels identified through sensing and analytical power estimations for the mesh operation.

The rest of this paper is organized as follows. In Section II, we list our assumptions and give an overview of the working of our proposed COMNET algorithms. In Section III, we lay out our analytical framework for spectrum sensing. Section IV presents our analytical model for calculating the interference due to neighboring mesh activity and Section V proposes a spectrum sharing algorithm based on this model. Our models are thoroughly evaluated in Section VI. Section VII describes the related work in this area and Section VIII discusses some issues related to our approach. Finally, we conclude our

work in Section IX while pointing out directions for further research.

## II. ARCHITECTURE AND SYSTEM OPERATION

The COMNET design aims to embed intelligent spectrum sensing capability in a standard mesh scenario without advanced hardware/software techniques such as (i) wideband filters that can sense bandwidth of several hundreds of MHz and (ii) the use of a priori knowledge of the sender's transmission content [1]. While these advancements, if present, will undoubtedly enhance cognitive radio operation, our aim is to use off-the-shelf components that are commercially available, like the legacy IEEE 802.11 WLAN cards operating in the secondary band. We now explain the mesh architecture that is used by our algorithms followed by an explanation of the working of the system.

### A. Architecture Description

As seen in Figure 1, a given mesh router (MR) has several clients (MCs) under it and these jointly form a *cluster*. The standard mesh network architecture consists of several such clusters, and all uplink/downlink flows are directed from the individual MCs towards its own MR and forwarded in a multihop fashion towards the gateway connected to the Internet. Each cluster can be visualized to be a single WLAN system, with the MR as the access point and the MCs as nodes served by it. Peer to peer communications between mesh clients belonging to different clusters may also be carried out without passing through the gateway.

Each MR and MC is equipped with a single IEEE 802.11 b based transceiver. Using typical assumptions of a frequency agile radio [1], this is tunable to any one of the allowed frequencies (channels) in the primary or the secondary band at a given time. This reduces the cost and complexity typically associated with two-transceiver nodes. In addition, the MRs are considered to be resource rich and can undertake computational overheads. MR-MR multi-hop links are achieved through out of band communication on a different channel, and is not subject to contention from the remaining nodes [2]. While the number of MCs in a cluster may change dynamically, each MR has a fixed location that is known to all the other MRs in the mesh system.

We assume the primary transmitters to be stationary radio/television towers in this work, and shall henceforth refer to them as primary stations. There is no restriction on the mobility of the primary receivers. As an indicative primary band, we consider 16 channels with 5 MHz spacing, and ranging from 712 – 787 MHz with similar transmission and power mask restrictions<sup>1</sup> as the ISM band. These values can be easily changed to suit any other band and network requirements in a specific primary user system.

Our algorithm requires an MC to calculate its distance from the primary stations when required. This cannot be accomplished by received signal strength (RSSI) calculations based on primary station power, as the received power in

<sup>1</sup>FCC imposed constraint on the leakage power as a function of distance from the center transmission frequency

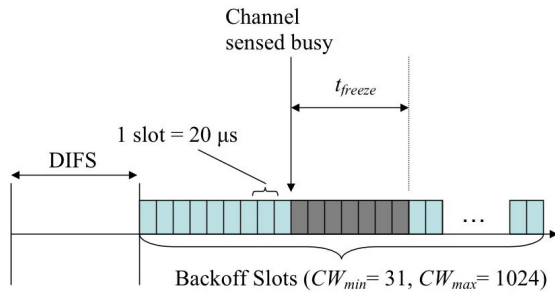


Fig. 2. The radio may switch to the primary channel for the duration of the packet transfer during the freeze duration, if it is not the intended recipient.

that band is a summation of several different transmitters whose frequencies are unknown. Instead, we use localization techniques like triangulation in the ISM band by tuning in succession to the MC's own channel and that of a neighboring cluster. As all occupied ISM channels and locations of the fixed MRs are known in advance, unlike in the primary band, the interference effects from other MRs can be accounted for in the calculation.

### B. System Operation

We now summarize the working of the system with an example scenario shown in Figure 1. The MCs periodically tune to a pre-decided channel in the primary band and sense the total received power for a short duration. These sensed values are communicated by the MCs, along with their distances from the primary stations, to the MRs of their respective clusters by piggybacking over data packets. However, in the event that only peer to peer communication exists in the network without involving the gateway, MRs need to send their statistics specially at a pre-decided frequency to it. Thus, MCs  $x'$ ,  $y'$  and  $z'$  in cluster  $C_1$  measure the received power on channel 9, say, and report it back to their MR. Each MR of a cluster then uses our proposed sensing solution, explained in Section III, to identify the primary station frequencies.

This information about the detected primary frequencies at a cluster is included in packets directed towards the gateway from the MRs, and updated in a centralized database at the gateway. This database also contains the number of active transmitting nodes in a cluster, which is easily obtained as every traffic stream from a given MC of a cluster passes through the gateway. The data tuple in the form of  $\langle \text{cluster ID, primary frequencies detected, number of nodes} \rangle$  for all the clusters in the network is included at regular intervals in the downstream packets from the gateway. This mechanism allows dissemination of the primary station data to all the clusters in the network, i.e.,  $C_1$ ,  $C_2$  and  $C_3$  in our example, without the use of additional packets or delays.

Based on these received values and our analytical model presented in Section IV, each MR can then calculate an approximate measure of interference introduced by its own cluster, as well as the others, at any arbitrary geographical location and channel. As each MR has the same input conditions and is

TABLE I  
SIMULATION PARAMETERS FOR THE 3 TRANSMITTER SCENARIO

Primary Tx	Distance from $x'$ (m)	Channel	Frequency (MHz)
1	230	9	752
2	230	9	752
3	500	13	772

subjected to the same constraints, they independently solve an optimization problem of deciding which of them should shift their operation in the primary band and the frequency that may be used in that band. Thus, clusters as a whole remain in the ISM band or switch to the primary band so that the network load is balanced, and the primary band interference is within allowed limits. In the event that  $C_1$  is identified as the cluster that must shift to the primary band, the MR and  $x'$ ,  $y'$ ,  $z'$  under it, must together change to a new frequency returned as a solution to the optimization problem. We next describe the problem of spectrum sensing, i.e., identifying the frequencies currently being used by primary stations, so that they may be avoided when a device shifts into the primary band.

### III. SPECTRUM SENSING

Our proposed method for channel sensing based on time domain sampling is outlined in Section III-A. We then apply it in centralized and distributed approaches in Sections III-B and III-C respectively.

#### A. Use of the backoff interval for channel sensing

At the physical layer (PHY), the IEEE 802.11 standard [25] provides a backoff timer that chooses a random number,  $r$ , in  $[0, CW]$ , where  $CW$  stands for contention window. The node sets the timer to the value  $20 \mu\text{s} \times r$  and counts down to zero as shown in Figure 2 after the completion of the time given by the Distributed Inter Frame Spacing (DIFS) [25]. Now, during this countdown interval, the channel is still sensed by the radio. If it is found busy at any particular slot, the backoff counter is frozen for the duration that the channel is found to be occupied. In our approach, the MC decodes the header at the MAC layer while the channel is still sensed busy by the PHY. If it is not the intended recipient of the packet, it does not need to monitor the channel any further for the duration specified in the header. The MC now switches to the primary channel for sensing the spectrum usage in that band. However, the classical approach of tuning individually to all available channels and gathering channel statistics has the following limitations:

- The short time duration for which the timer is frozen poses an upper limit on the number of channels that may be sensed in succession. Assuming the sensing time in each channel is  $20 \mu\text{s}$ , the channel switching time may range from  $100 \mu\text{s}$  to  $200 \mu\text{s}$  for real devices [14]. Figure 3(a) shows the number of channels that may be sampled by a single node during one packet transmission time. We see that for low packet sizes like 512 bytes and the typically used 11 Mbps link, less than 3 channels can be sampled indicating the inadequacy of direct sampling,

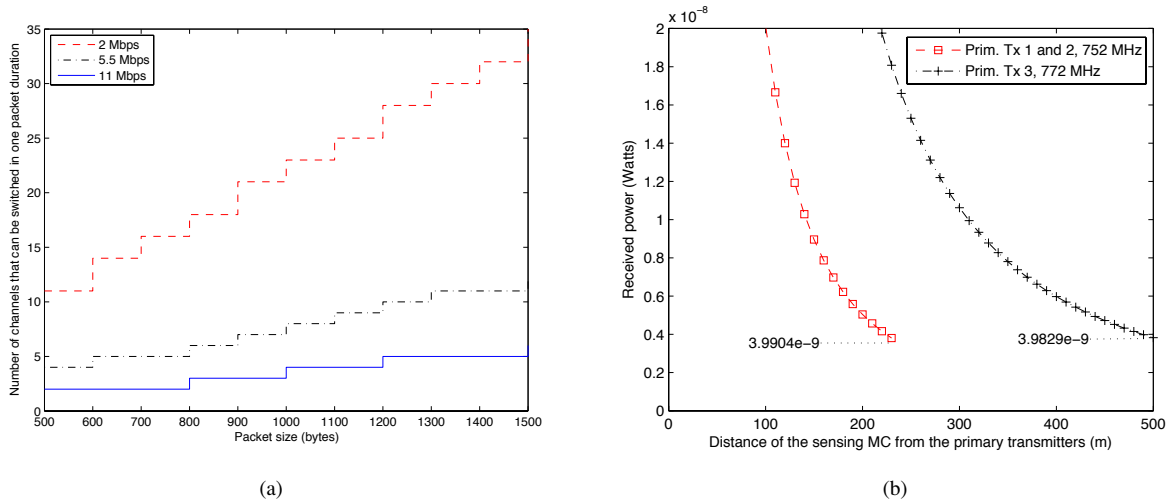


Fig. 3. The number of channels that can be sensed in a single duration for which the timer is frozen, for varying packet sizes and transmission rates is shown in (a). When received power is measured at channel 772 MHz, the combined effect of two primary stations 1 and 2 is the same as the single transmitter 3 (b).

especially when large number of channels are present. This can be alleviated to an extent by assigning the task of monitoring subsets of the available primary channels to different MCs. This approach too suffers from scalability issues and requires further coordination by the MR.

- Estimating the channel occupancy by received signal power alone may not guarantee accurate results. As an example, as shown in Figure 4, consider MC  $x'$  sensing the primary band when primary stations 1, 2 and 3 are active. Their assigned frequencies and distances are shown in Table I. When the received power is measured at MC  $x'$ , at channel 13, the effect of a single transmitter 3 on that channel is the same as the combined action of 1 and 2 on different channels (Figure 3(b)). Thus, it cannot be said with certainty whether a given channel is indeed occupied based on an isolated signal strength measurement in that channel.

Our approach is hence motivated by the need to develop spectrum sensing techniques that can gather channel information for the entire band by sampling only a single channel without any tradeoffs in scalability, as is shown in the next section.

### B. Centralized framework for time-domain sensing

We recall that an MC tunes to a single pre-decided primary channel and senses the received power for the entire duration available. This is essentially a superposition of the received power due to several transmitters. These transmitters may be on different channels, and only a small proportion of their transmit power leaks into the channel in which the measurement is done. Thus, this leakage power is a function of the separation between the channels used for transmission and measurement. If the channel for measurement is fixed, and the leakage power for each transmitter is isolated from the aggregate received power, then the individual transmitter channels can be estimated.

We assume a simple free space path loss model and that all primary stations use the same transmit power. From Figure 4,

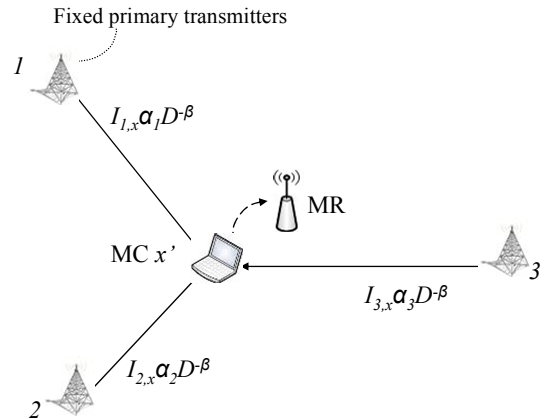


Fig. 4. MC  $x'$  senses the channel when three primary stations are in the neighborhood. The received power is the sum of the individual transmit powers scaled by the spectral overlap factor.

the average normalized power received on channel  $f_{x'}$  at node  $x'$  due to primary station 1 on channel  $f_1$  only, when separated by a distance  $D_{1,x'}$  is given by,

$$P_{1,x'} = I_{1,x'} \cdot \alpha_1 D_{1,x'}^{-\beta} \quad (1)$$

Here,  $\alpha_1 = \frac{G_t G_r c^2}{(4\pi f_1)^2}$ , where  $G_t$  and  $G_r$  are the transmit and receiving antenna gains, and  $c$  is the speed of light.  $I_{1,x'}$  is the spectral overlap factor between the channels of transmitter and receiver, and is either made available as standard data or can be calculated through power mask requirements [4]. It is the proportion of the original transmit power that gets leaked into the channel used for measurement.

The received power,  $P_{x'}$  at node  $x'$ , due to  $M$  primary stations is merely the superposition of the individual received powers due to each of them (Figure 4) and hence,

$$\begin{aligned} P_{x'} &= \sum_{i=1}^M I_{i,x'} \cdot \alpha_i D_{i,x'}^{-\beta} \\ &= I_{1,x'} \cdot \alpha_1 D_{1,x'}^{-\beta} + I_{2,x'} \cdot \alpha_2 D_{2,x'}^{-\beta} + \dots + I_{M,x'} \cdot \alpha_M D_{M,x'}^{-\beta} \end{aligned} \quad (2)$$

TABLE II  
SPECTRAL OVERLAP AS A FUNCTION OF CHANNEL SEPARATION

$\Omega$ Values	0	1	2	3	4	5	6
Spectral Overlap	1	0.8	0.5	0.2	0.1	0.001	0

Similarly, if any  $M$  MCs out of the total number in a cluster measure the transmitted power due to  $M$  different primary stations, the received power  $P_i$  at each of them can be written as,

$$\begin{aligned} P_1 &= I_{1,1} \cdot \alpha_1 D_{1,1}^{-\beta} + \dots + I_{M,1} \cdot \alpha_M D_{M,1}^{-\beta} \\ P_2 &= I_{1,2} \cdot \alpha_1 D_{1,2}^{-\beta} + \dots + I_{M,2} \cdot \alpha_M D_{M,2}^{-\beta} \\ &\vdots \\ P_M &= I_{1,M} \cdot \alpha_1 D_{1,M}^{-\beta} + \dots + I_{M,M} \cdot \alpha_M D_{M,M}^{-\beta} \end{aligned} \quad (3)$$

As each MC tunes to the same channel for sensing, the fractional power overlap between its own channel and that of any one primary station is the same for all of them. As an example, with respect to the primary station at channel 1 and using the same notation as in equation (1), for MCs 1, 2, ...,  $M$ , we have  $I_{1,1} = I_{1,2} = I_{1,3} = \dots = I_{1,M}$ . We can express this precisely as follows: Let the set of primary stations as  $U_P$  and the set of MCs of a given cluster be represented as  $\mathbb{C}$ . As all the MCs tune to the same channel, for any such two of them,  $i$  and  $j$ , the power overlap is the same with a given primary station. Thus,

$$If \ i = k, \ I_{i,j} = I_{k,l} \quad \forall i, k \in U_P, j, l \in \mathbb{C} \quad (4)$$

However, the channel adds a finite noise  $\eta$  to the ideal power ( $P_{ideal} = P_{x'}$ ) in equation (2) to give the true received power ( $P_{true} = P_{ideal} + \eta$ ). Though we describe the ideal case, the error introduced as a result of this simplification and addressed by undertaking noise correcting measures are explored in Section VI. Using (4), we can now express the set of equations in (3) in the matrix form  $\mathbf{DX} = \mathbf{Y}$ ,

$$\begin{bmatrix} D_{1,1}^{-\beta} & D_{2,1}^{-\beta} & \dots & D_{M,1}^{-\beta} \\ D_{1,2}^{-\beta} & D_{2,2}^{-\beta} & \dots & D_{M,2}^{-\beta} \\ \vdots & \vdots & \ddots & \vdots \\ D_{1,M}^{-\beta} & D_{2,M}^{-\beta} & \dots & D_{M,M}^{-\beta} \end{bmatrix} \begin{bmatrix} I_{1,1} \alpha_1 \\ I_{2,1} \alpha_2 \\ \vdots \\ I_{M,1} \alpha_M \end{bmatrix} = \begin{bmatrix} P_1 \\ P_2 \\ \vdots \\ P_M \end{bmatrix} \quad (5)$$

Here, the distances of each of the primary stations (represented by matrix  $\mathbf{D}$ ) is known to the MCs measuring the received signal power, as discussed earlier. The column vector  $\mathbf{Y}$  is the received signal power, inclusive of noise. Hence, we can solve for  $\mathbf{X}$  as,  $\mathbf{X} = \mathbf{D}^{-1} \mathbf{Y}$ . For each entry  $i$  of the column vector  $\mathbf{X}$ , substituting  $\alpha$  and assuming gains  $G_t = G_r = 1$  we can write,

$$I_{i,1} \cdot \alpha_i = \phi_i \quad (6)$$

$$I_{i,1} \frac{c^2}{(4\pi f_i)^2} = \phi_i \quad (7)$$

We estimate the channel frequency  $f_i$  that minimizes the error between the observed and the calculated values as shown in (8). The spectral overlap factor is formally expressed as a

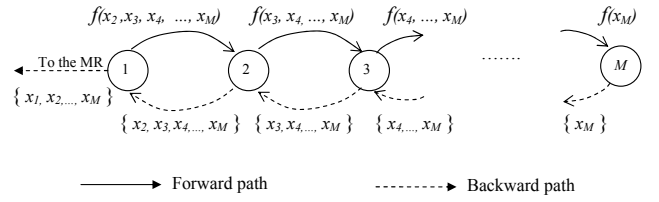


Fig. 5. Each hop reduces the number of variables by 1 and forwards it to the next hop. The return path is initiated at the  $M^{th}$  node, and each time, all the solved values of the variables obtained are sent to the previous hop. This continues till all the unknowns are solved and finally communicated to the MR.

function,  $\Omega$ , of channel separation in (9), where  $\Delta f$  is the inter-channel spacing.

$$f_i = \arg_k \min \left[ I_{k,1} \frac{c^2}{(4\pi f_k)^2} - \phi_i \right] \quad (8)$$

$$I_{i,1} = \Omega \left( \frac{|f_i - f_1|}{\Delta f} \right) \quad (9)$$

As an example, sample values for  $\Omega$ , for IEEE 802.11b with  $\Delta f = 5$  MHz, are listed in Table II. These values are obtained through empirical measurements using two Linux laptops equipped with NETGEAR MA401 802.11b wireless cards in an indoor setting and found to be in accordance with analytical values in [4]. As the center frequencies of the primary channels are known *a priori*, and  $f_1$  is pre-decided, the best fit can be easily computed in (8). The prediction accuracy can be increased by introducing noise correction factors and averaging results obtained from a number of sets of such linear equations. We explore the benefits and tradeoffs of these approaches in Section VI.

### C. Distributed approach to sensing

In this section we modify the centralized scheme so that the cost of computation is equally shared amongst all the  $M$  MCs. This approach is analogous to a distributed implementation of the classical Gauss elimination technique for solving linear equations [17].

We begin by substituting the variable  $x$  for the spectral overlap factor  $I$  and  $\alpha$  from the path loss model defined in equation (1),

$$x_i = I_{i,j} \cdot \alpha_i \quad \forall i \in U_P, j \in \mathbb{C} \quad (10)$$

Substituting  $x_i$  in (3), and using the relation between the spectral overlap factors defined in (4), the power received at MCs 1, 2, ...,  $M$  is given by,

$$P_1 = x_1 D_{1,1}^{-\beta} + x_2 D_{2,1}^{-\beta} + \dots + x_M D_{M,1}^{-\beta} \quad (11)$$

$$P_2 = x_1 D_{1,2}^{-\beta} + x_2 D_{2,2}^{-\beta} + \dots + x_M D_{M,2}^{-\beta} \quad (12)$$

$\vdots$

$$P_M = x_1 D_{1,M}^{-\beta} + x_2 D_{2,M}^{-\beta} + \dots + x_M D_{M,M}^{-\beta} \quad (13)$$

Now, expressing (11) in terms of  $x_1$ ,

$$x_1 = P_1 \left( \frac{1}{D_{1,1}} \right)^{-\beta} - x_2 \left( \frac{D_{2,1}}{D_{1,1}} \right)^{-\beta} + \dots - x_M \left( \frac{D_{M,1}}{D_{1,1}} \right)^{-\beta} \quad (14)$$

TABLE III  
DESCRIPTION OF THE NEW FIELDS ADDED IN THE HEADER

Field	Description
Dest_MC	The next hop node along the chain that should overhear the packet
X_Values	Variables of the set of linear equations calculated till current MC
Equation	Equation obtained by eliminating 1 variable as shown in (14)
Hops	Number of hops to be completed

In (14), we have managed to express  $x_1$  in terms of the  $(M - 1)$  other variables. This is basically the step of elimination of a single variable in the Gauss elimination method. The expression for  $x_1$  can be now substituted in (12) which now has a total of  $(M - 1)$  unknowns. In the next iteration, we write  $x_2$  in terms of the other  $(M - 2)$  variables,  $x_3, \dots, x_M$ , thus eliminating a second unknown. Thus, at the end of  $(M - 1)$  such iterations, we are left with a single variable that is trivially solved, say  $x_M$ . This value can now be substituted in the expression for  $x_{M-1}$ , which we recall, is a function of a single unknown variable,  $x_M$ . This process of backtracking by re-substituting and obtaining the value of a new unknown is carried on till the value of  $x_1$  is obtained, in a manner similar to the classical Gauss elimination technique.

In the practical implementation, the information required for solving the equations hop-by-hop is inserted in the MAC header through the additional fields listed in Table III. Each MC reduces the number of variables by 1 and forwards the new expression in the field Equation to its one-hop neighbor identified in Dest\_MC. Note that nodes still continue to direct their traffic towards the MR as before, but now also snoop on the header field to identify whether they are the intended next hop in the distributed sensing process. This continues till a chain of  $M$  MCs is formed, as shown in Figure 5. At the  $M^{th}$  node, the value of  $x_M$  is trivially obtained, which is then propagated backwards along the chain. Each hop along the backward path now solves for one variable and forwards all other values received by it, in the field X\_Values, to the preceding MC. When the MC that initiated the chain finally receives the backtracking packet on the reverse path, it sends the estimated channel values to the MR. This distributed scheme performs exactly similar to the centralized one, but at an additional time cost associated with the forwarding and backtracking operations along a chain of  $M$  nodes.

While sensing is used to locate empty portions of the spectrum, it is necessary to evaluate the additional power injected before actually shifting the secondary users in the primary band. For this, we propose an analytical model for estimating interference caused at any arbitrary location and frequency due to the mesh traffic.

#### IV. ANALYTICAL INTERFERENCE MODEL

In this section, we develop an analytical model for the total power received at a given location due to a nearby WLAN activity. This allows each MR to solve the optimization problem discussed in Section V for band/channel assignment

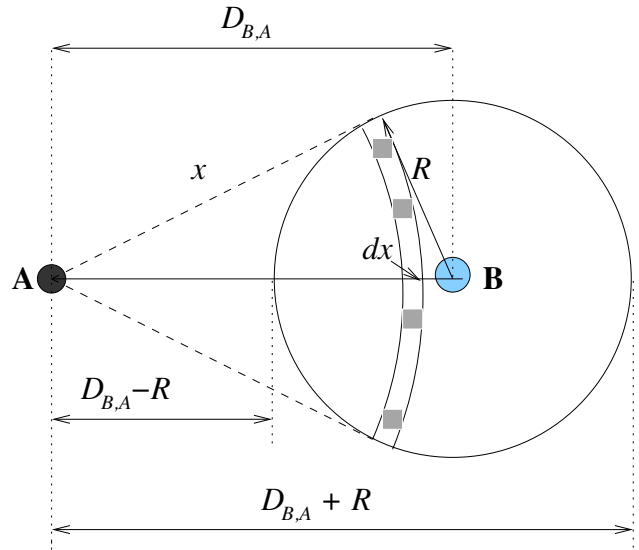


Fig. 6. Calculation of received power at user located at A due to a cluster of  $N$  nodes under MR B.

TABLE IV  
SYMBOLS USED IN THE ANALYTIC APPROXIMATION OF RECEIVED POWER

Symbol	Description
$\sigma$	Single slot duration ( $20 \mu\text{sec}$ )
$\tau$	Probability of transmission in a single slot
$p_{tr}$	Probability at least one node transmitting in a cluster
$m$	Maximum value of the backoff stage
$W$	Minimum value of the contention window
$p$	Packet collision probability
$N$	Total nodes in a sample cluster
$\rho$	Node density in a cluster
$D_{i,j}$	Distance of location $j$ from cluster $i$
$R$	Transmission radius of the MR
$T_{pkt}$	Average transmission duration
$T_{total}$	Average time for which channel is occupied, inclusive of sensing times
$t_p$	Time taken to transmit data packet
$t_a$	Time taken to transmit ACK
$H$	Time taken to transmit MAC header
$T_s$	Channel busy time under successful packet transmission
$T_c$	Channel busy time under packet collision

independently, while arriving at the same solution. For ease of representation, the important symbols used in the subsequent discussion are summarized in Table IV.

Under the assumption that all transmitting nodes are in saturation and using the same notations as in [5], the stationary probability that a station transmits in a generic time slot is defined as  $\tau$ , which is in turn, a function of the packet collision probability  $p$ . Derived in [5], (15) and (16) formally establish these relations while (17) gives the probability of at least one

station transmitting in the WLAN cluster.

$$\tau = \frac{2}{1 + W + pW \sum_{i=1}^{m-1} (2p)^i} \quad (15)$$

$$p = 1 - (1 - \tau)^{N-1} \quad (16)$$

$$p_{tr} = 1 - (1 - \tau)^N \quad (17)$$

The instantaneous transmitted power  $E[P_x]$  from a given number of nodes can then be derived from the following theorem.

*Theorem 1:* The instantaneous power transmitted by  $n$  nodes in a small considered strip in the WLAN coverage area, in any given slot, each with maximum transmission power  $P_{tx}$  is given by  $E[P_x] = P_{tx} n \tau$ .

*Proof:* Proof is included in the Appendix. ■

In order to calculate the total received power at a given point  $A$ , we first consider the trivial case of one cluster. The MR  $B$  for that cluster is at a distance  $D_{B,A}$  away from it (Figure 6) with a coverage radius of  $R$ . We assume that  $N$  MCs are distributed uniformly around MR  $B$ , in circle of radius  $R$ . We also observe that the MCs associated with MR  $B$  are at a closest distance of  $D_{B,A} - R$  and at the furthest distance of  $D_{B,A} + R$  from  $A$ . The node density is  $\rho = \frac{N}{\pi R^2}$  in the area covered by the cluster with  $B$  as its MR. Consider a thin strip of infinitesimal width  $dx$  as shown at a distance  $x$  from  $A$ . The length of arc  $\widehat{l}_{a,b}$  and the area under the strip is,

$$\begin{aligned} \widehat{l}_{ab} &= x \cdot 2\theta \\ dA_{ab} &= \widehat{l}_{ab} dx = x \cdot 2\theta dx \end{aligned} \quad (18)$$

The number of nodes in this area is hence given by,

$$dA_{ab} \rho = \rho x \cdot 2\theta dx \quad (19)$$

Applying the Cosine rule to  $\Delta AaB$ , we get,

$$\theta = \arccos\left(\frac{x^2 + D_{B,A}^2 - R^2}{2xD_{B,A}}\right) \quad (20)$$

From Theorem 1 and equation (19), the power contributed by the strip is,

$$dP = P_{tx} \tau \rho \times 2x\theta dx \quad (21)$$

We assume that the received power is measured at a user located at  $A$ , tuned to a frequency  $f_A$ . We use the same path loss formula described earlier in equation (1) that scales down the received power by accounting for spectral overlap between transmitter and receiver frequencies.

Also, from substituting from equation (20) and using  $\Psi = I_{B,A} 2\alpha P_{tx} \tau \rho$ , we get the received power at location  $A$  as,

$$dP_{dx,A}(f_B, f_A) = \Psi \cdot x^{1-\beta} \cos^{-1}\left(\frac{x^2 + D_{B,A}^2 - R^2}{2xD_{B,A}}\right) dx \quad (22)$$

Hence, we get the instantaneous power contribution of all nodes under MR  $B$ ,  $P_{B,A}^{f_B, f_A}$ , by integrating over the circle

defined by its transmission radius.

$$\begin{aligned} P_{B,A}^{f_B, f_A} &= \int_{D_{B,A}-R}^{D_{B,A}+R} dP_{dx,A}(f_B, f_A) dx \\ &= \Psi \cdot \int_{D_{B,A}-R}^{D_{B,A}+R} x^{1-\beta} \cos^{-1}\left(\frac{x^2 + D_{B,A}^2 - R^2}{2xD_{B,A}}\right) dx \end{aligned} \quad (23)$$

We note that the channel may be idle for several slots in a given interval and hence the expression for instantaneous power needs to be averaged over time. Under the basic scheme, each node of the cluster may either transmit a data packet directed at the MR or send an ACK in response to an incoming packet from the MR. Thus, the average duration for the transmission,  $T_{pkt}$ , given the probability that at least one transmission has occurred, is

$$T_{pkt} = p_{tr} \left(\frac{t_p + t_a}{2}\right) \quad (24)$$

where  $t_p$  and  $t_a$  are the times taken to transmit a data packet and an ACK respectively.

Here, we do not distinguish between successful transmission and collision conditions as our aim is to calculate the total received power for all cases. In the event of a collision, the node completes transmitting all the bytes of a message and then suffers an ACK timeout. This timeout duration,  $T_c$ , is the same as that taken for a successful transmission,  $T_s$ , in the basic access scheme. Along the lines of [5], the time duration to complete one data transfer inclusive of the sensing times and receiving a reply is,

$$T_{total} = (1 - p_{tr})\sigma + p_{tr}T_s + p_{tr}T_c \quad (25)$$

where according to our assumptions, and ignoring propagation times,

$$T_s = T_p \quad (26)$$

$$T_s = H + DIFS + t_p + t_a + SIFS$$

Here,  $DIFS$  is defined earlier in Section III-A and SIFS is the Short Inter Frame Spacing [25]. Thus, the average received power  $P_{avg}^{f_B, f_A}(B, A)$  sensed by user located at  $A$  on channel  $f_A$  due to a mesh cluster centered at  $B$ , using channel  $f_B$  can be calculated using (23), (24) and (25) as,

$$P_{avg}^{f_B, f_A}(B, A) = P_{B,A}^{f_B, f_A} \times \frac{T_{pkt}}{T_{total}} \quad (27)$$

Let  $U_S$  be set of all the clusters in the region. Now, the total received power seen by the user at  $A$  due to all the clusters  $i, i \in U_S$  can be derived by summing up their individual average power contributions obtained from equation (27).

$$P_{A-total} = \sum_{\forall i \in U_S} P_{avg}^{f_A, f_i}(i, A) \quad (28)$$

Having obtained an analytical model that gives the power received at a given location and frequency, each MR can estimate the effect of the other clusters without explicit messaging. This allows the formulation of a decentralized channel allocation scheme described in Section V.

TABLE V  
SYMBOLS USED IN THE ILP

Symbol	Description
$U_P$	Set of primary stations
$U_S$	Set of all mesh based clusters
$U_S^p$	Set of clusters shifted to the primary band
$U_S^s$	Set of clusters remaining in the unlicensed band
$I_{i,j}(f_i, f_j)$	Spectral overlap at location $i$ between frequency $f_i$ and transmitter frequency $f_j$
$P_{i,j}$	Received power at location $i$ due to transmitter $j$ at frequency $f_j$
$B$	Set of numbered blocks, of side $l$
$F$	Set of possible primary channels

## V. THE BAND AND CHANNEL SWITCHING ALGORITHM

In this section, we use the models developed in Sections III and IV to develop a scheme that allows shifting some of the clusters into the primary band so that the network load is shared equally between the primary and secondary bands. These clusters must also be allotted operating frequencies that introduce tolerable interference in the primary band, while considering the already occupied channels identified through sensing in Section III. We model this as an Integer Linear Program (ILP) [3] that must satisfy load sharing and interference constraint equations.

As discussed in Section II, the inputs in our problem formulation are the primary frequency information and the number of transmitting nodes in a cluster. This is disseminated through the downstream packets to all the clusters served by the gateway. The optimization problem described next is solved at each MR and as the same constraints and inputs are present with all of them, they independently arrive at the same solution.

We assume that the extent of the region in which the radios operate is known, and without loss of generality this is taken as a square of side  $\mathbb{L}$  units. This square is further divided into blocks each of length  $l$ , which are then numbered from  $1, \dots, l^2$ . The received power at a particular block is measured at the center of the block. We now formulate the ILP by using the notations explained in Table V.

Given :  $U_P, U_S, f_i \forall i \in U_P, F, B, I$

To find :  $U_S^p, f_j \quad \forall j \in U_S^p$  (29)

Subject to :

$$\sum_{j \in U_P, f_j \neq f_i} P_{i,j} I_{i,j}(f_i, f_j) + \sum_{k \in U_S^p} P_{i,k} I_{i,k}(f_i, f_k) < T_{th}, \quad \forall i \in B, \forall f_i \in F \quad (30)$$

$$\sum_{k \in U_S^p} P_{i,k} - \sum_{q \in U_S^s} P_{i,s} < P_{th}, \quad \forall i \in B \quad (31)$$

$$||U_S^p| - |U_S^s|| < N_{th} \quad (32)$$

From (29), we observe that the parameters to be found are (i) the clusters that shift to the primary band, and (ii) their operating frequencies. However, this choice has to be made in such a way that the total interference caused by the currently transmitting primary stations and the clusters newly introduced

in the band must be within permissible bounds for each of the primary channel frequencies, and throughout the region of interest.

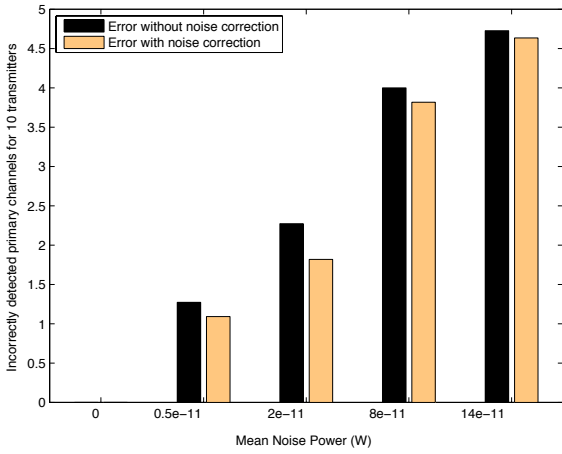
- The constraint (30) ensures that total interference power from the primary stations (indicated by the first summation) and the shifted clusters (second summation term) is checked against a threshold  $T_{th}$  for each block in the region, and again for all the primary band frequencies for that block. Here, we exclude the cases where the primary frequency that is being checked for in a block is already being used by a primary station.
- The desired aim of shifting some of the clusters into the primary band is to balance the network load between the primary and secondary bands for the mesh system. Thus, the total interference power contributed by the clusters in the two bands is divided in (31) in a manner that the difference in network load, measured as the function of the difference in their received power for all blocks, is within a threshold  $P_{th}$ . For the purpose of calculation, the transmit frequencies of all the clusters are fixed to a pre-determined channel in the secondary band.
- In order to avoid a single dominant cluster from shifting into the primary band, we also balance the number of clusters in the two bands in (32) through the cluster difference threshold,  $N_{th}$ .

The solution that adheres to this set of constraints balances the network load in the two bands and also allocates the channels for the secondary users. If the decision to switch a channel is taken, then the MR intimates the MCs in its cluster. The channel to be switched to and the time after which the new channel will be active is included in this information. In the current implementation, the clusters revert back to the secondary band after a time-out period and further intelligent re-assignment schemes can be developed over this framework.

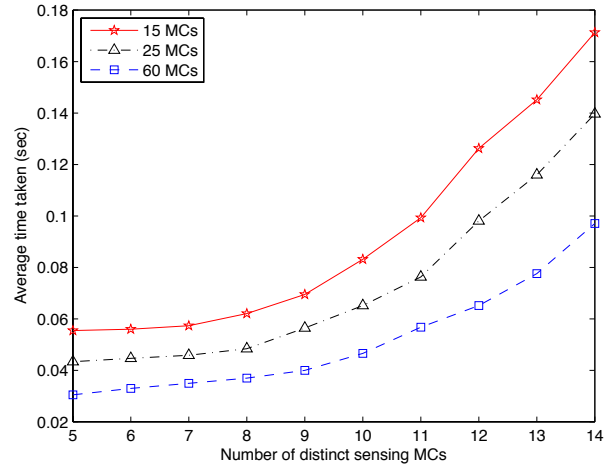
## VI. PERFORMANCE EVALUATION

In this section, we first present simulation results to validate the models proposed in Sections III and IV. We then demonstrate the advantages of the proposed load distribution scheme discussed in Section V with the associated overheads.

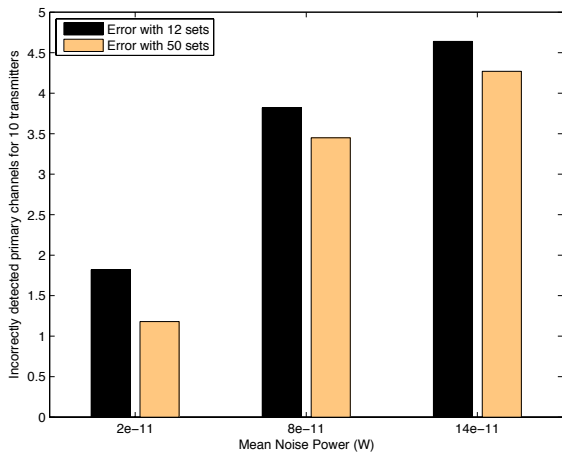
We used the J-Sim simulator [24] for our study. Each MC of a cluster is driven into saturation by generating UDP packets with an inter-arrival time of  $10^{-4}$  seconds. The MAC layer is IEEE 802.11b at 11 Mbps with the RTS/CTS handshaking mechanism disabled for the basic access scheme. The packets generated are each of 512 bytes at the MAC layer, which after inclusion of the MAC PLCP header and preamble attains a total size of 598 bytes. We account for the fact that the PHY preamble is always transmitted at 1 Mbps while calculating the total duration for which the received power is observed. The transmission radius of the MR is considered as 150 meters, and the entire region of study is limited to a square of side 900 meters. The antenna gains are assumed unity, the transmission power for both the primary and secondary stations is 0.1 Watts, and the path loss exponent,  $\beta$  is taken as 2. The primary band structure is described in Section II-A. The



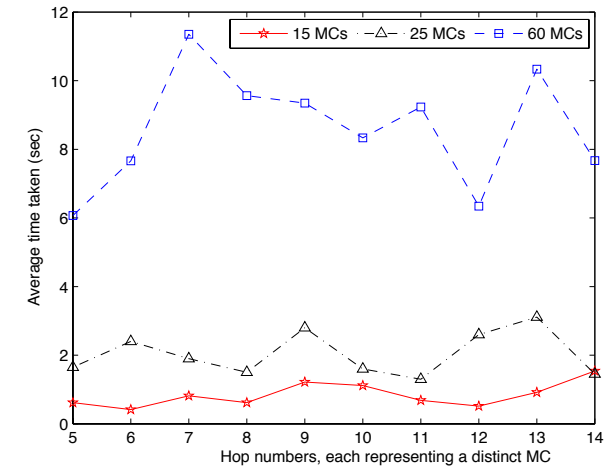
(a)



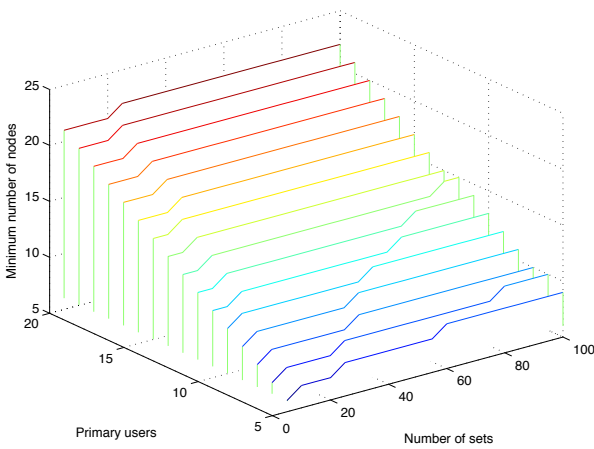
(a)



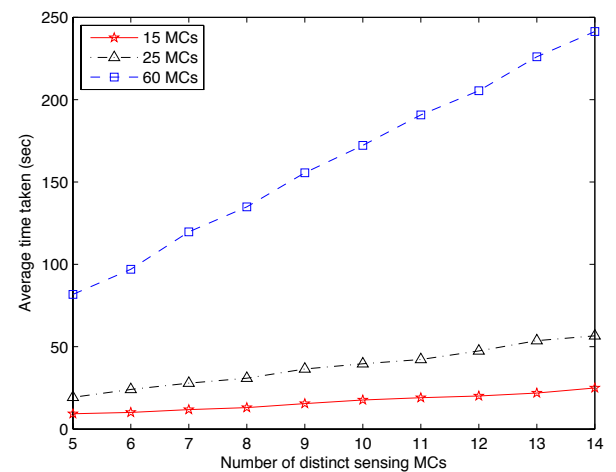
(b)



(b)



(c)



(c)

Fig. 7. Effect of noise power on the accuracy of the analytically predicted frequencies used by the primary stations, for a constant number of sets (a) and the improvement in accuracy of prediction of the channels used by the primary stations with increasing number of sets (b). Graph (c) shows the relationship between the number of minimum required sensing nodes, for a given number of required sets and primary stations.

Fig. 8. The time overhead for the centralized (a) and distributed (c) schemes is compared. The time taken at each hop of the chain propagation for the distributed approach is shown in (b).

optimization problem presented in Section V was implemented in AMPL [9], and solved with CPLEX [23].

### A. Spectrum Sensing

In order to study the accuracy of the spectrum sensing method proposed in Section III, we uniformly distributed 10 continuously operational primary stations for one run of the simulation, and averaged over 50 such trials. Again, each transmitter was randomly assigned any one of 16 possible channels in the primary band. A single cluster of 40 MCs was considered, and these nodes were distributed uniformly in the transmission region of its MR.

Figure 7(a) shows the effect of increasing noise powers on the accuracy of the channel frequency estimation. The noise is modeled as a Gaussian distributed variable with varying means and a standard deviation of  $0.25 \times 10^{-11}$ . Typically, the noise power with a mean of  $2 \times 10^{-11}$  Watts is considered high and we show performance results upto the extreme case of  $14 \times 10^{-11}$  Watts. As expected, the sensing accuracy of the system decreases with increasing ambient noise. We have evaluated both the naive scheme wherein the receiver has no knowledge of the channel noise and when a constant mean noise value is subtracted from each of the received power readings. We call the latter approach as *noise correction* in which this constant mean value of noise is obtained through ambient noise sampling or provided beforehand based on the environment of deployment. Our sensing scheme identifies the primary channels correctly when noise is neglected and suffers about 10% inaccuracy under the moderate channel noise value of  $0.5 \times 10^{-11}$  Watts.

The sensing results can be improved as shown in Figure 7(b) by taking several sets of measurements, and considering the primary station frequencies detected maximum number of times. This performance improvement, as an example by 22% under high noise conditions of  $2 \times 10^{-11}$  Watts, comes at a computation cost as several sets of 10 linear equations needs to be solved each time. These results can also be used to compute the probability of incorrect detection for varying noise powers and measurement sets by dividing the channels in error by the total number of primary stations in the network.

The relationship between the number of primary stations ( $M$ ), the user defined metric of number of sets that determines accuracy ( $S$ ), and the minimum required sensing MCs ( $n$ ), is shown in Figure 7(c). This graph is computed as follows: We need a minimum of  $n$  sensing MCs such that we can generate a new set of  $M$  linear equations by choosing  $M$  nodes out of  $n$  each time. As  $S$  sets are required,  ${}^n C_M = S$ . We observe that the minimum MCs needed for a given number of sets scales nearly linearly with the increasing number of primary stations. However, there is no significant overhead introduced in terms of the number of nodes communicating their sensed values even for a very large number of sets. From the observed values, we see that even for 100 sets, with 20 independently transmitting primary stations, 22 sensing MCs are sufficient.

We next compare the time overhead of the centralized sensing scheme (Section III-B) with the distributed scheme (Section III-C) in clusters of varying sizes. We define the latency metric as the time taken by the minimum required number of MCs to sense the channel power and communicate these values to the MR. The low latency of the centralized scheme as seen in Figure 8(a) makes its suitable for dynamic

primary networks, though at a higher computational complexity at the MR. For the distributed scheme, the MCs piggyback information for 1-hop neighbors on the data packets directed to the MR. We modified the IEEE 802.11 MAC header in J-Sim to include the additional fields specified in Table III. The distributed approach involves the formation of chains of MCs, and the link level delay measured at each hop, from hop number 5 to 14 is shown in Figure 8(b). When repeated for different cluster sizes, results reveal that this delay gets larger with increasing nodes owing to progressively greater contention. This has a direct bearing on the total time taken to complete a full round of communication comprising of propagating packets forward and backward along the chain. For a single such chain, from Figure 8(c), we observe that there is a high time overhead with increasing cluster nodes. This problem can be alleviated by adopting a flexible next hop approach, instead of rigidly binding a specific node in the DEST\_MC field. This will allow any node in receiving distance to undertake the next stage of Gauss elimination, and we leave further investigation in this direction as future work.

### B. Validation of the analytical model for received power estimation

Our proposed model for estimating the received power at a given location due to WLAN cluster is validated by varying (i) the number of nodes in the cluster to 7 and 25, (ii) the distance between the MR and the chosen location, and (iii) the transmit power used. We observe from Figure 9(a) that the analytical results are in good agreement with the simulation ones, and become more accurate with the increasing distance. This is because at the ratio of the transmission radius  $R$  to the measurement distance  $D$  decreases, the circular source region (Figure 6) appears to shrink and in the limiting case, i.e., at infinite distance, it becomes a point source. Thus, the dependency on the approximation obtained by integrating over the entire circle defined by  $R$  decreases with increasing distance, giving accurate results. Figure 9(a) also shows that the model is a better representation of the cluster when the node density is high. The power received from the cluster of 25 nodes is better estimated than that of 7 nodes as more nodes result in a truly uniform distribution over the entire circle defined by  $R$ .

Figure 9(b) measures the effect of changing transmission power on the power received at the chosen location. We observe that the system behaves linearly, and again, the estimate proves to be better for larger number of nodes.

### C. Performance of the band/channel selection algorithm

In order to verify the benefits of the band switching and channel allocation algorithm described in Section V, we consider a sample topology as shown in Figure 11. The thresholds  $T_{th}$ ,  $P_{th}$ , and  $N_{th}$  are empirically chosen as  $4 \times 10^{-9}$  Watts,  $2.2 \times 10^{-10}$  Watts, and 2 respectively, given the network size. It is possible to have a finer control over this algorithm by tuning these parameters according to desired performance constraints. The triangles represent 25 node clusters in the considered area of  $900 \times 900 m^2$  with the MRs at the marked positions. The squares indicate the fixed stationary primary stations.

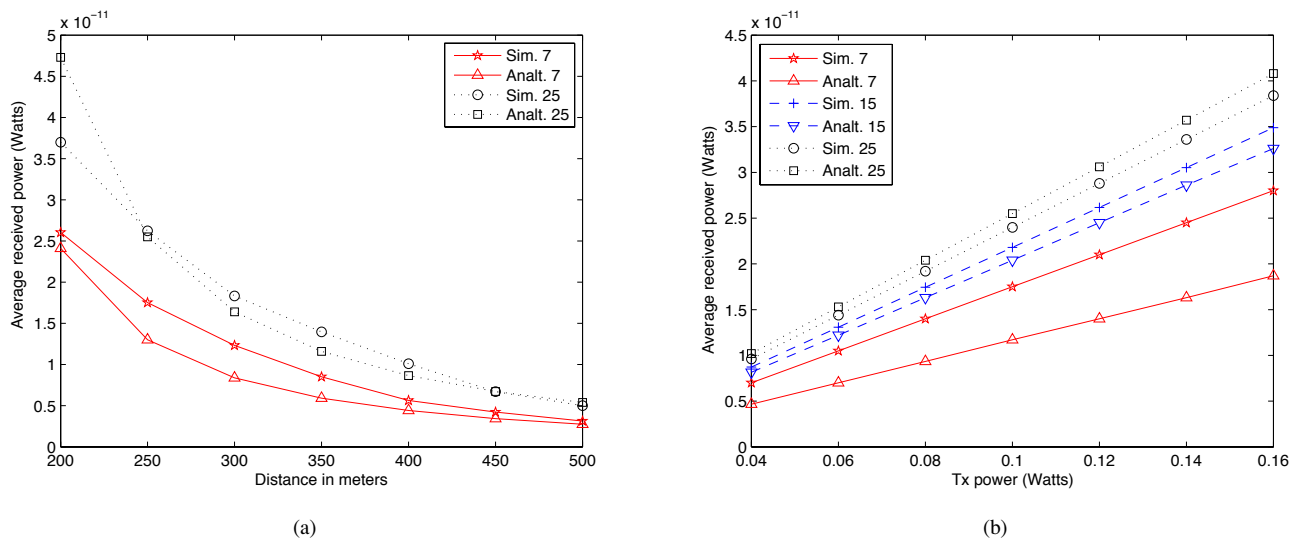


Fig. 9. The analytical model presented in Section IV is verified for increasing distance (a) and transmit power (b).

Both of these are uniquely identified in their respective bands by the ID in the superscript. Similarly, the channel number is indicated in the parenthesis, also in the subscript. Note that two network components may have the same channel number but lie in different bands, like cluster 1 and primary station 1. Their individual transmission channels are, however, centered at 2412 MHz and 712 MHz respectively and thus they coexist without affecting each other. The clusters, when in the secondary band, and the primary stations are assigned channels in the best possible manner, so that their individual operation is not affected by the others<sup>2</sup>. Some of these clusters (2, 3, and 6), move into the primary band as a result of the solution computed for the optimization problem in Section V. Their new channel numbers in this band are indicated in square brackets in the subscript. For the subsequent discussion and power measurements, we consider the central region of the area marked by the coordinate (450, 450).

We observe in Figure 10(a) that the power in the primary channels due to cluster activity is located in the portions of the spectrum which are comparatively free of the effect of primary station transmissions. Channels 9–12 already experience high power leakage from the ongoing transmission on channel 11, and are avoided by our channel allocation algorithm, making it sensitive to primary station activity. We next compare the simulation and analytical values for the received power in the secondary band before (Figure 10(b)) and after the execution of the optimization problem (Figure 10(c)). Even when the original channel assignment was optimally best, after shifting three clusters in the primary band, each channel now experiences reduced leakage power due to spectral overlap. Additionally, we observe that the total power seen in all the channels in the secondary band is approximately halved, indicating good load balancing between the bands. These results also serve in validating the received power predicted by the analytical model in Section IV in a more general scenario.

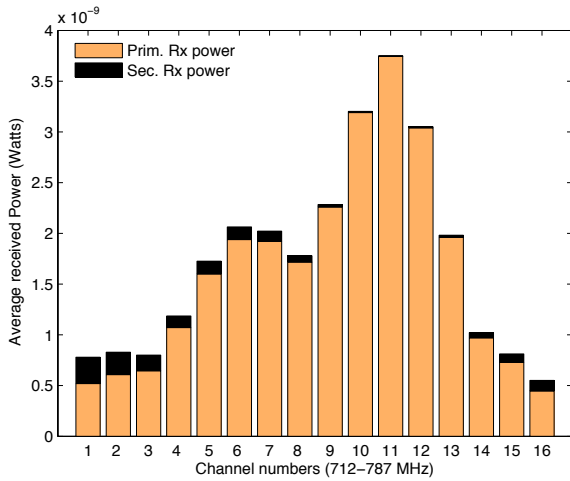
<sup>2</sup>Channels 1, 6, 11 are considered to be totally non-overlapping and the carrier sense threshold is double of the transmission radius,  $R$ , taken as 150 meters.

## VII. RELATED WORK

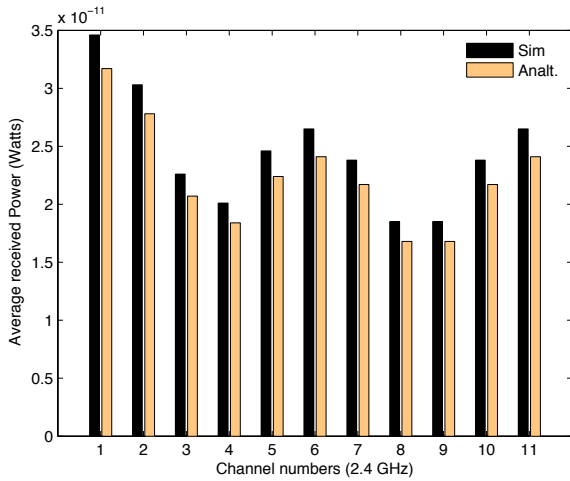
Most sensing techniques can be classified into *single user* detection and *cooperative* detection. The former can be achieved by either simply sensing the energy over time in a channel and comparing with a threshold [6][18] or by leveraging primary user information like modulation type, pulse shape, packet format [18]. Our approach is along the lines of [10][20], in which information from multiple sources is used cooperatively to estimate channel usage leading to a lower rate of false negatives. However, the work presented in [10] is limited in applicability as it addresses the special case of two users and a single primary transmitter using a TDMA like protocol. An auxiliary sensor network solely responsible for sensing is deployed in [20], thus making its realization difficult in practical scenarios.

An interesting solution to the problem of sensing uses interference as a tool for gathering channel information. The term *interference temperature limit* is defined for receivers in [8], in which the aggregate sum of all RF power must be below this cap to be classified as noise. Though we incorporate this measure in our optimization solver, our sensing algorithm uses the power spectral leakage in adjacent channels at the transmitter. This is fundamentally different from the detector proposed in [21] where the local oscillator leakage power emitted by the RF front-end is used for detection.

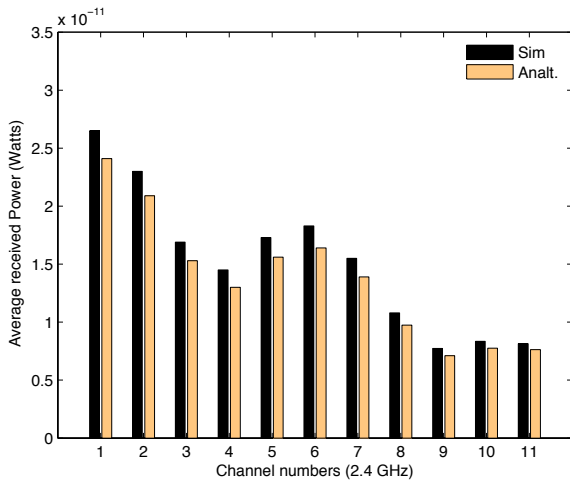
Analogous to the spectrum sensing, spectrum sharing techniques have been investigated in cooperative [22][16] and non-cooperative or selfish approaches [19]. In the former method, interference measurements are collected from the sensing devices and this information is shared amongst the others during detection. Our work follows the assumptions in [16], in which, primary transmitter locations and transmit power are assumed to be known and the solution is modeled as an optimization problem. However, [16] considers a flat topology and is limited to spectrum allocation amongst secondary users, as primary user constraints are not included. Thus, it can be used to supplement our proposed approach by allocating a fresh set of channels to the clusters that remain in the



(a)



(b)



(c)

Fig. 10. The received power in each of the 16 channels of the primary band for the primary and secondary transmitters is shown in (a). The received power at each of the 11 channels of the secondary band at the central location is shown before (b) and after (c) the shift of the clusters 2, 3 and 6, into the primary band.

secondary band. Non-cooperative solutions perform less better

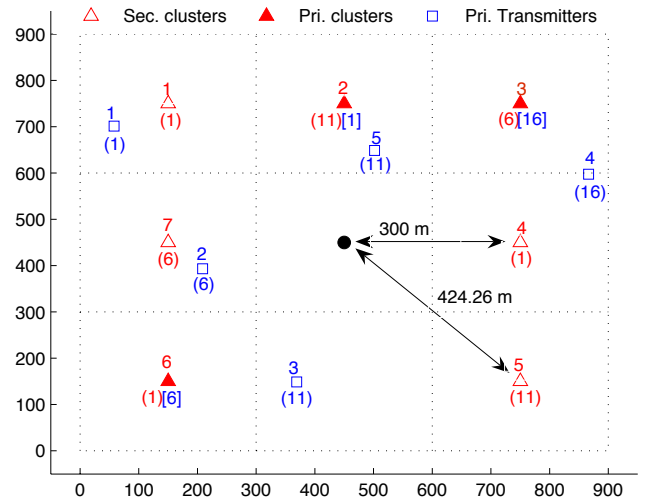


Fig. 11. The topology considered for investigating the gains obtained through the band/channel shifting scheme.

as they use only localized information, but significantly reduce time and energy expended in disseminating sensed values. Recently, game theoretic analysis has also been used wherein it is shown that cooperative approaches can be modeled as an exact potential game, with a fast converging Nash equilibrium solution [15]. Bargaining is another related technique which used to solve this problem [22]. However, most game theoretic approaches need periodic interaction between the *players* or the spectrum sensing devices, and thus incur a high communication overhead.

### VIII. DISCUSSION

Our work attempts to describe the functioning of a WMN in a cognitive radio environment. While we have tried to address the practical concerns to the best of our knowledge, this section lists some issues that can be further improved upon and qualifies them in light of the assumptions made in this paper.

- We assume stationary primary transmitters in the form of television and radio broadcast towers. As television/radio stations are well defined and towers have precise locations, it is possible to have an accurate fix on primary user coordinates. Future work in this direction would be to incorporate primary user mobility in the proposed algorithm framework. Note that secondary user mobility does not affect our approach as the sensing process is typically completed in a single packet transmission duration (few hundred microseconds). This short time period does not translate to large physical displacement that may cause a perceptible change in the signal strength.
- For purposes of modelling, we have assumed a saturation condition at each MC, where a node always has a packet to send. This is true for most Internet applications involving use of multimedia and file upload/download operations. We are in process of extending this work to non-saturated conditions as well, which may account for low or sporadic traffic conditions.

- In the current approach, the values sensed by any  $M$  MCs may be used for determining used primary channels. However, as each MC experiences different ambient noise levels, a biased selection may help in improving the estimation accuracy.
- Our work assumes a lookup table that gives the fractional overlap in the primary station channels, i.e. how much power is leaked into a given channel when transmission occurs in any other channel in the same band. This can be easily obtained through a one-time offline measurement or as standard data published by the primary user. In this work we have assumed similar band structure and spectral overlap in the primary band as in the ISM band, as this data is readily available. Our work can be modified to suit any other primary user network by appropriately changing Table II and the transmit power.

## IX. CONCLUSIONS

Our proposed COMNET solution suite integrates cognitive radio functionalities in a WMN architecture. A novel spectrum sensing method is proposed that allows identifying primary user frequencies without additional transceivers and changing the de facto IEEE 802.11 standard for WMNs. We have also devised an analytical model to estimate power received at point due to a cluster operation in its neighborhood, which is used to decide channel and band allocations. Though we have addressed specifically the concerns of wireless mesh networking, our solutions can be easily applied to other general purpose ad-hoc networks. As other complex optimization techniques for channel usage like adaptive modulation, rate control, power control, amongst others, are devised, they can be incorporated transparently to the operation of the COMNET algorithms. Our distributed approach for channel selection makes our scheme scalable and is specially considerate of primary station interference tolerances. Future work consists of using unsaturated traffic models and extending this protocol suite to the network and transport layers. Thus, the spectrum allocation and management functions can be combined with end-to-end congestion and reliability parameters, or routing schemes can be devised that choose the next hop based on primary station activity in the area. We envisage an integrated networking solution that will necessarily be cross-layered and have cognitive abilities embedded at every stage.

## ACKNOWLEDGMENT

This material is based upon work supported by the US National Science Foundation under Grant No: CNS-07251580.

## APPENDIX A

### PROOF OF THEOREM 1

*Proof:* Let the probability of  $i$  simultaneous transmissions be denoted by  $p_i$ , where,

$$p_i = {}^n C_i \tau^i (1 - \tau)^{n-i} \quad (33)$$

Note that this is different from the expression for packet collision probability  $p$  in equation (16). Now, the expected value of the transmitted power is,

$$E[P_{tx}] = p_1 P_{tx} + p_2 2P_{tx} + p_3 3P_{tx} + \dots + p_n n P_{tx} \quad (34)$$

From (33) and (34), we get,

$$\begin{aligned} E[P_{tx}] &= \sum_{i=1}^n {}^n C_i \tau^i (1 - \tau)^{n-i} i P_{tx} \\ &= {}^n C_1 \tau (1 - \tau)^{n-1} P_{tx} + {}^n C_2 \tau^2 (1 - \tau)^{n-2} 2P_{tx} + \dots + \\ &\quad \tau^n n P_{tx} \end{aligned} \quad (35)$$

In order to simplify (35), consider the expression for binomial expansion,

$$(p + q)^n = {}^n C_1 p q^{n-1} + {}^n C_2 p^2 q^{n-2} + \dots + {}^n C_n p^n$$

Differentiating *w.r.t*  $p$ , and multiplying with  $p P_{tx}$ , i.e.,

$$\begin{aligned} p P_{tx} \frac{d}{dx} (p + q)^n &= p P_{tx} {}^n C_1 q^{n-1} + 2p P_{tx} {}^n C_2 p^1 q^{n-2} + \dots + \\ &\quad p P_{tx} n {}^n C_n p^{n-1} \end{aligned} \quad (36)$$

Substituting  $p = \tau$  and  $q = 1 - \tau$  in equation (36),

$$P_{tx} n \tau = {}^n C_1 \tau (1 - \tau)^{n-1} P_{tx} + {}^n C_2 \tau^2 (1 - \tau)^{n-2} 2P_{tx} + \dots + \tau^n n P_{tx} \quad (37)$$

Comparing (35) and (37), we see that  $E[P_{tx}] = P_{tx} n \tau$ . ■

## REFERENCES

- [1] I. F. Akyildiz, W. Y. Lee, M. C. Vuran, and S. Mohanty. NeXt Generation/Dynamic Spectrum Access/Cognitive Radio Wireless Networks: A Survey. *Elsevier Computer Networks Journal*, 50:2127–2159, September 2006.
- [2] I. F. Akyildiz, X. Wang, and W. Wang. Wireless mesh networks: a survey. *Elsevier Computer Networks Journal*, 47(4):445–487, November 2005.
- [3] R. K. Ahuja, T. L. Magnanti, and J. B. Orlin. *Network Flows: Theory, Algorithms, and Applications*. Prentice Hall, Englewood Cliffs, New Jersey, February 1993.
- [4] A. Mishra, V. Shrivastava, S. Banerjee, and W. Arbaugh. Partially overlapped channels not considered harmful. *ACM SIGMETRICS Perform. Eval. Rev.*, 34(1):63–74, 2006.
- [5] G. Bianchi. Performance analysis of the IEEE 802.11 DCF. *IEEE Journal on Selected Areas of Communications*, 18(3):535–547, March 2000.
- [6] F. Digham, M. Alouini, and M. Simon. On the Energy Detection of Unknown Signals Over Fading Channels. *IEEE Trans. on Communications*, 55(1):21–24, January 2007.
- [7] FCC Spectrum Policy Task Force. Report of spectrum efficiency working group. [Online]. Available: First note and Order, Federal Communications Commission, ET-Docket 98-153, Adopted February 14, 2002, released April 22, 2002.
- [8] FCC Spectrum Policy Task Force. Report of spectrum efficiency working group. ET Docket No 03-237 Notice of Inquiry and Notice of Proposed Rulemaking .
- [9] R. Fourer, D. M. Gay, and B. W. Kernighan. *AMPL: A Modeling Language for Mathematical Programming*. Duxbury Press / Brooks/Cole Publishing Company, 2002.
- [10] G. Ganesan and Y. G. Li. Cooperative Spectrum Sensing in Cognitive Radio Networks. In *Proc. of IEEE International Symposium on Dynamic Spectrum Access Networks*, pages 137–143, November 2005.
- [11] P. Gupta and P. R. Kumar. The Capacity of Wireless Networks. *IEEE Trans. on Information Theory*, 46(2):388–404, March 2000.
- [12] Joseph Mitola III. Cognitive Radio: An Integrated Agent Architecture for Software Defined Radio. Ph.D Thesis, KTH Royal Institute of Technology, 2000.
- [13] P. Kyasanur and N. H. Vaidya. Capacity of multi-channel wireless networks: Impact of number of channels and interfaces. In *Proceedings of ACM MobiCom 2005*, Cologne, Germany, August 2005.
- [14] J. Mo, H. S. W. So, and J. Walrand. Comparison of Multi-channel MAC Protocols. In *Proc. 8th ACM international symposium on Modeling, analysis and simulation of wireless and mobile systems*, pages 209–218, New York, NY, USA, 2005.

- [15] N. Nie and C. Comaniciu. Adaptive Channel Allocation Spectrum Etiquette for Cognitive Radio Networks. In *Proc. of IEEE International Symposium on Dynamic Spectrum Access Networks*, pages 269–278, November 2005.
- [16] C. Peng, H. Zheng, and B. Y. Zhao. Utilization and Fairness in Spectrum Assignment for Opportunistic Spectrum Access. *ACM Mobile Networks and Applications (MONET)*, 11(4):555–576, 2006.
- [17] William H. Press, William T. Vetterling, Saul A. Teukolsky, and Brian P. Flannery. *Numerical Recipes in C++: the art of scientific computing*. 2002.
- [18] A. Sahai, N. Hoven, and R. Tandra. Some Fundamental Limits in Cognitive Radio. In *Proc. of Allerton Conf. on Commun., Control and Computing 2004*, October 2004.
- [19] S. Sankaranarayanan, P. Papadimitratos, A. Mishra, and S. Hershey. A Bandwidth Sharing Approach to Improve Licensed Spectrum Utilization. In *Proc. of IEEE International Symposium on Dynamic Spectrum Access Networks*, pages 279–288, November 2005.
- [20] S. Shankar. Spectrum Agile Radios: Utilization and Sensing Architecture. In *Proc. of IEEE International Symposium on Dynamic Spectrum Access Networks*, pages 160–169, November 2005.
- [21] B. Wild and K. Ramchandran. Detecting Primary Receivers for Cognitive Radio Applications. In *Proc. of IEEE International Symposium on Dynamic Spectrum Access Networks*, pages 124–130, November 2005.
- [22] J. Zhao, H. Zheng, and G.-H. Yang. Spectrum Agile Radios: Utilization and Sensing Architecture. In *Proc. of IEEE International Symposium on Dynamic Spectrum Access Networks*, pages 259–268, November 2005.
- [23] CPLEX solver. [Online]. Available: <http://www.cplex.com>.
- [24] J-Sim Network Simulator. <http://www.j-sim.org/>.
- [25] IEEE Std 802.11b-1999/Cor 1-2001, 2001.
- [26] Specification of the bluetooth system - version 1.1b, specification volume 1 & 2. Bluetooth SIG, February 2001.



**Ian F. Akyildiz** (M'86-SM'89-F'96) received the B.S., M.S., and Ph.D. degrees in Computer Engineering from the University of Erlangen-Nuernberg, Germany, in 1978, 1981 and 1984, respectively.

Currently, he is the Ken Byers Distinguished Chair Professor with the School of Electrical and Computer Engineering, Georgia Institute of Technology, Atlanta, and Director of Broadband Wireless Networking Laboratory. He is an Editor-in-Chief of *Computer Networks Journal (Elsevier)* as well as the founding Editor-in-Chief of the *AdHoc Network Journal (Elsevier)* and the *Physical Communication Journal (Elsevier)*.

His current research interests are in cognitive radio wireless networks, wireless sensor networks, and wireless mesh networks.

He received the "Don Federico Santa Maria Medal" for his services to the Universidad of Federico Santa Maria, in 1986. From 1989 to 1998, he served as a National Lecturer for ACM and received the ACM Outstanding Distinguished Lecturer Award in 1994. He received the 1997 IEEE Leonard G. Abraham Prize Award (IEEE Communications Society) for his paper entitled "Multimedia Group Synchronization Protocols for Integrated Services Architectures" published in the IEEE Journal of Selected Areas in Communications (JSAC) in January 1996. He received the 2002 IEEE Harry M. Goode Memorial Award (IEEE Computer Society) with the citation "for significant and pioneering contributions to advanced architectures and protocols for wireless and satellite networking". He received the 2003 IEEE Best Tutorial Award (IEEE Communication Society) for his paper entitled "A Survey on Sensor Networks," published in IEEE Communications Magazine, in August 2002. He also received the 2003 ACM Sigmobile Outstanding Contribution Award with the citation "for pioneering contributions in the area of mobility and resource management for wireless communication networks". He received the 2004 Georgia Tech Faculty Research Author Award for his "outstanding record of publications of papers between 1999-2003". He also received the 2005 Distinguished Faculty Achievement Award from School of ECE, Georgia Tech. He has been a Fellow of the Association for Computing Machinery (ACM) since 1996.



**Kaushik R. Chowdhury** received his B.E. degree in Electronics Engineering with distinction from VJTI, Mumbai University, India, in 2003. He received his M.S. degree in computer science from the University of Cincinnati, OH, in 2006, graduating with the best thesis award. He is currently a Research Assistant in the Broadband Wireless Networking Laboratory and pursuing his Ph.D. degree at the School of Electrical and Computer Engineering, Georgia Institute of Technology, Atlanta, GA. His current research interests include cognitive radio architectures, and

resource allocation in wireless multimedia sensor networks. He is a student member of IEEE.